



The combined immunohistochemical expression of AMBRA1 and SQSTM1 identifies patients with poorly differentiated cutaneous squamous cell carcinoma at risk of metastasis: A proof of concept study

Michael H. Alexander^{1,2,3}  | William J. Cousins^{1,2} | Tom Ewen^{1,2}  | Andrew P. South³ | Penny Lovat^{1,2} | Niki Stefanos⁴

¹Translational and Clinical Research Institute, Newcastle University, Newcastle upon Tyne, UK

²AMLo Biosciences, Newcastle Helix, Newcastle upon Tyne, Newcastle upon Tyne, UK

³Department of Dermatology and Cutaneous Biology, Thomas Jefferson University, Philadelphia, Pennsylvania, USA

⁴Cellular Pathology, Addenbrookes Hospital, Cambridge, UK

Correspondence

Michael H. Alexander, Department of Dermatology and Cutaneous Biology, Thomas Jefferson University, Philadelphia, PA 19107, USA.
Email: michael.alexander2@jefferson.edu

Present address

Niki Stefanos, Cellular Pathology, Jersey General Hospital, Jersey, UK.

Funding information

Northern Powerhouse; AMLo Biosciences; European Regional Development Fund

Abstract

Background: Cutaneous squamous cell carcinoma (cSCC) incidence continues to increase globally with, as of yet, an unmet need for reliable prognostic biomarkers to identify patients at increased risk of metastasis. The aim of the present study was to test the prognostic potential of the combined immunohistochemical expression of the autophagy regulatory biomarkers, AMBRA1 and SQSTM1, to identify high-risk patient subsets.

Methods: A retrospective cohort of 68 formalin-fixed paraffin-embedded primary cSCCs with known 5-year metastatic outcomes were subjected to automated immunohistochemical staining for AMBRA1 and SQSTM1. Digital images of stained slides were annotated to define four regions of interest: the normal and peritumoral epidermis, the tumor mass, and the tumor growth front. H-score analysis was used to semi-quantify AMBRA1 or SQSTM1 expression in each region of interest using Aperio ImageScope software, with receiver operator characteristics and Kaplan–Meier analysis used to assess prognostic potential.

Results: The combined loss of expression of AMBRA1 in the tumor growth front and SQSTM1 in the peritumoral epidermis identified patients with poorly differentiated cSCCs at risk of metastasis (* $p < 0.05$).

Conclusions: Collectively, these proof of concept data suggest loss of the combined expression of AMBRA1 in the cSCC growth front and SQSTM1 in the peritumoral epidermis as a putative prognostic biomarker for poorly differentiated cSCC.

KEYWORDS

autophagy, biomarker, cSCC

This is an open access article under the terms of the [Creative Commons Attribution-NonCommercial-NoDerivs](https://creativecommons.org/licenses/by-nc-nd/4.0/) License, which permits use and distribution in any medium, provided the original work is properly cited, the use is non-commercial and no modifications or adaptations are made.

© 2024 AMLo Biosciences Ltd. *Journal of Cutaneous Pathology* published by John Wiley & Sons Ltd.

1 | INTRODUCTION

Cutaneous squamous cell carcinoma (cSCC) is a malignancy arising from the cancerous transformation of squamous keratinocytes, the predominant cellular component of the epidermis. The global incidence of cSCC is steadily increasing, with a recent study demonstrating an increase in 27 countries worldwide between 1990 and 2007.¹ Despite this rise in global incidence, surgical excision of cSCC remains largely curative.^{2,3} However, for those patients who develop advanced disease, prognosis is poor, with an almost 50% rate of recurrence and a 10-year survival rate of <20%.⁴

Histopathological features have been shown to correlate with an increased risk of metastasis, including a poorly differentiated phenotype, perineural invasion, and a tumor dimension >4 cm; however, alone, none of these clinical-pathological features display reliable prognostic accuracy.⁵ Collectively, these data highlight the acute unmet need for credible biomarkers to identify patient subsets with an increased risk of metastasis.

Considerable efforts have been made to develop prognostic biomarkers, however, the high mutational burden and heterogeneity in cSCC has limited the potential for genetic-based biomarkers. Whilst genetic tests exist, protein-based biomarkers may more accurately reflect the metabolic expression of the tumor cells and serve as more powerful prognostic biomarkers.⁶⁻¹⁰

Recently, the immunohistochemical expression of regulatory proteins of autophagy, the cellular process that sequesters cytoplasmic contents or organelles for degradation, has been identified as valuable prognostic biomarkers for cutaneous malignancies.¹¹ In cancer, autophagy plays a paradoxical role, with a blockade in activity accelerating mutagenesis in early carcinogenesis, while more advanced-stage tumors use autophagy to facilitate survival in nutrient/oxygen-poor environments.¹² Under normal physiological states, autophagy, and its sister process nucleophagy, also contribute to epidermal differentiation, allowing keratinocytes to fully flatten and elongate before cornification.^{13,14} Given the active role of autophagy in ensuring the complete differentiation of keratinocytes and that loss of its activity promotes carcinogenesis, autophagy regulatory proteins may serve as prognostic biomarkers for cutaneous malignancies.

AMBRA1 is an autophagy regulatory protein that, in nutrient-rich conditions, sequesters BECLIN 1-VPS34 into a complex on dynein light chain 1/2, preventing autophagosome nucleation and the progression of autophagy.¹⁵ Studies of the immunohistochemical expression of AMBRA1 in the epidermis overlying early-stage melanoma have shown loss of expression in combination with the non-continuous expression of Loricrin in the stratum corneum, identifies patients at higher risk of disease progression.^{11,16} Furthermore, loss of expression of the autophagy cargo protein SQSTM1 has also been identified as a prognostic biomarker in several solid tumors, including melanoma.¹⁷ Under normal cellular homeostasis, SQSTM1 interacts with ubiquitinated proteins, shuttling them to the expanding autophagosome to ensure degradation, with reduced SQSTM1 expression indicative of the exploitation of autophagy to extend tumor cell life.^{18,19} Studies have also shown that SQSTM1 activity contributes to

the reprogramming of the tumor microenvironment, altering lipid distribution and metabolic rates in adipose cells and activating Nrf2 in cancer-associated fibroblasts.^{20,21}

Given that both AMBRA1 and SQSTM1 act as autophagy regulatory proteins and the already established link between their expression and carcinogenesis, their expression, either alone or in combination, may act as a prognostic biomarker. This prompted the current proof of concept study aimed at developing a methodology to quantify AMBRA1 and SQSTM1 expression, determining their potential to identify high-risk cSCC subsets and their potential relationship with other risk factors, including tumor differentiation status.

2 | MATERIALS AND METHODS

2.1 | Discovery cohort of primary cSCCs

A retrospective cohort of 68 formalin-fixed paraffin-embedded (FFPE) primary cSCCs, with known metastatic outcomes, were obtained from the Tissue Biobank, Addenbrookes Hospital, Cambridge University Hospitals NHS Foundation Trust (Table 1). The time to disease metastasis (months) for each case was extrapolated from pathology reports, from the dates of the surgical excision of the primary and any metastatic tumor. Full ethical permission for this study was obtained through the Newcastle University Dermatology Biobank (REC REF 19/NE/004_Lovat) and a material transfer agreement with the Tissue Biobank, Addenbrookes Hospital, Cambridge.

2.2 | Quantitative immunohistochemical analysis of AMBRA1 and SQSTM1 expression

FFPE sections (4 μ m) from primary cSCCs were adhered to charged glass slides and subjected to automated immunohistochemistry (IHC) staining for AMBRA1 and SQSTM1 expression. Antigen retrieval conditions and primary antibody dilutions for AMBRA1 (AbD33473; AMLo Biosciences) and SQSTM1 (sc-28359; Santa Cruz) were optimized using a Ventana Benchmark XT automated IHC staining instrument (Ventana Medical Systems, Inc.) with antibody binding visualized either with an Optiview DAB Detection Kit (Ventana Medical Systems, Inc.), an ultraView Universal DAB Detection Kit (Ventana Medical Systems, Inc.) or a Discovery Fast Red detection kit (Ventana Medical Systems, Inc.) as previously described.²³

Quantification of AMBRA1 and SQSTM1 expression was determined via H-score analysis,²⁴ using Aperio ImageScope Software (Leica Biosystems). For all cSCC sections, four regions of interest were identified: the normal epidermis, the peritumoral epidermis, the tumor mass, and the tumor growth front. The normal epidermis was defined as the epidermal region adjacent to the peritumoral epidermis and extending over a distance of 1 mm or more with no evidence of dysplasia. The peritumoral epidermis was defined as the epidermis immediately adjacent to the cSCC, extending for a distance of up to 1 mm from the tumor, with or without, at most mild dysplasia. The tumor

TABLE 1 Patient cohort demographics.

Age	
≤60	7
>60	61
Sex	
Male	48
Female	20
Differentiation status	
Well	22
Moderately	26
Poorly	20
AJCC stage	
Stage I	36
Stage II	5
Stage III	17
Stage IV	10
BWH stage	
BWH 1	33
BWH 2A	24
BWH 2B	10
BWH 3	1
Metastatic status	
No metastasis	53
Metastasis	15
pT stage	
Stage I	42
Stage II	6
Stage III	19
Stage IV	1
Tumor size	
Unclassifiable	2
≤20 mm	54
>20 mm	12
Tumor thickness	
Unclassifiable	4
≤6 mm	41
>6 mm	23
Tumor depth	
Unclassifiable	6
≤6 mm	49
>6 mm	13
Perineural invasion	
Unclassifiable	6
Not present or present <0.1 mm	55
Present ≥0.1 mm or clinically significant	7
Immune status	
Compromised	30
Uncompromised	38

Note: Patients were considered immune compromised if there was a history of lymphoma/other cancer or if they were organ transplant recipients. Patients were categorized as metastatic if they had the presence of in-transit or nodal metastases. Tumor thickness and tumor depth categories were selected based on the 8th edition UICC guidelines.²² cSCC cases were sourced from all anatomical sites except those involving the eyes, eyelids, vulva, penis, perineal skin, and the vermilion surface of the lips.

growth front was defined as the infiltrative edge of the invasive tumor and no more than three cell layers in absolute thickness into the tumor mass, while the tumor mass was defined as the rest of the invasive lesion. For the normal and peritumoral epidermal regions of interest, two areas adjacent to the tumor were defined and annotated in detail. For both the tumor mass and tumor growth front, 1 mm² boxes were used to define five areas for each region, respectively. Following this, all tumor material present within the 1 mm² boxes underwent detailed annotation (Figure 1). The cytoplasmic H-score of AMBRA1 or SQSTM1 expression was determined in each annotated cSCC using the ImageScope cytoplasmic V2 algorithm, pre-optimized for analysis of keratinocyte/cSCC staining (Figures S1 and S2; Tables S1 and S2). The H-score for each region of interest for each cSCC was derived from the mean score of all staining across all annotated areas.

2.3 | Statistical analysis

All statistical analysis was performed using GraphPad Prism 9 (version 9.3.1). Statistical differences in cytoplasmic AMBRA1 and SQSTM1 expression levels between different cSCC regions of interest were determined by either a Mann–Whitney or an unpaired *t*-test, following a determination of data normality by a Shapiro–Wilk test.

The prognostic potential of cytoplasmic AMBRA1 or SQSTM1 expression in each region of interest was determined using receiver operator characteristic (ROC) analysis, with the region of interest with the area under the curve (AUC) value closest to one selected as the region with the highest prognostic potential. ROC values were also used to determine the cut-off value for high- and low-risk staining levels.

The ability of cytoplasmic AMBRA1 or SQSTM1 expression in each region to predict cSCC metastasis was assessed using Kaplan–Meier survival analysis, with the statistical separation of the populations determined using a log rank (Mantel–Cox) test.

3 | RESULTS

3.1 | AMBRA1 and SQSTM1 expression individually are unable to independently prognose cSCC metastasis

The prognostic utility of AMBRA1 and SQSTM1 in predicting cSCC metastasis was assessed in a discovery cohort of 53 non-metastatic and 15 metastatic primary cSCC cases comprising well, moderate, and poorly differentiated subtypes (Table 1). Following automated immunohistochemical staining for AMBRA1 and SQSTM1, and the acquisition of digital images from each case, all images were fully annotated with the mean cytoplasmic H-score for each potential biomarker derived in four discrete areas; the normal epidermis (representing an internal control for homeostatic epidermal AMBRA1 and SQSTM1 expression), peritumoral epidermis, tumor mass, and tumor growth front (Figure 1).

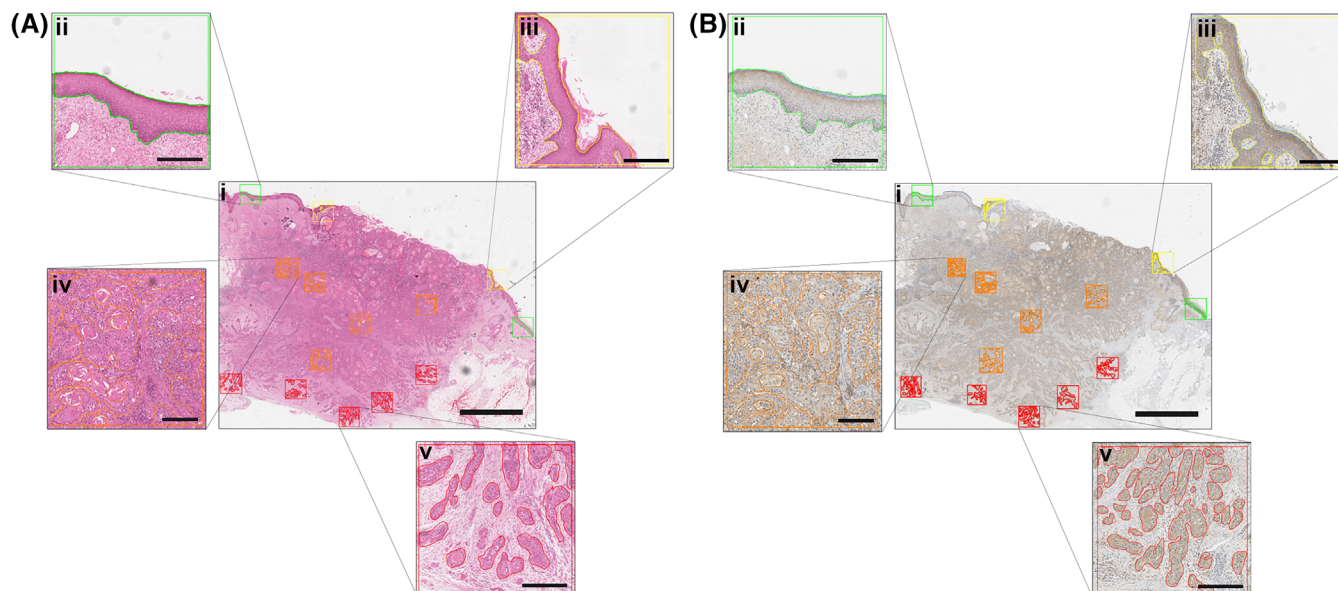


FIGURE 1 Digital annotation methodology used to analyze the expression of AMBRA1 and SQSTM1 in primary cutaneous squamous cell carcinoma (cSCC) tumors. (Ai) Representative photomicrograph image of a hematoxylin and eosin (H&E)-stained cSCC tumor with the respective annotations of normal epidermis (green), peritumoral epidermis (yellow), tumor mass (orange), and tumor growth front (red). (Aii) Enlarged photomicrograph image of the normal epidermis annotated region of the H&E-stained cSCC tumor. (Aiii) Enlarged photomicrograph image of the peritumoral epidermis annotated region of the H&E-stained cSCC tumor. (Aiv) Enlarged photomicrograph image of the tumor mass annotated region of the H&E-stained cSCC tumor. (Av) Enlarged photomicrograph image of the tumor growth front annotated region of the H&E-stained cSCC tumor. (Bi) Representative photomicrograph image of a cSCC tumor stained for AMBRA1 with the respective annotations of normal epidermis (green), peritumoral epidermis (yellow), tumor mass (orange), and tumor growth front (red). (Bii) Enlarged photomicrograph image of the normal epidermis annotated region of the AMBRA1-stained cSCC tumor. (Biii) Enlarged photomicrograph image of the peritumoral epidermis annotated region of the AMBRA1-stained cSCC tumor. (Biv) Enlarged photomicrograph image of the tumor mass annotated region of the AMBRA1-stained cSCC tumor. (Bv) Enlarged photomicrograph image of the tumor growth front annotated region of the AMBRA1-stained cSCC tumor. Visible staining was achieved via immunohistochemistry with a DAB counterstain. Image A/Bi was taken using bright-field microscopy with a magnification of $\times 0.8$. Scale bar = 3 mm. Image A/Bii–iv were taken using bright-field microscopy with a magnification of $\times 9.5$. Scale bar = 300 μm . Image A/Bv was taken using bright-field microscopy with a magnification of $\times 10.3$. Scale bar = 200 μm .

Statistical analysis of differences in mean cytoplasmic AMBRA1 expression between these areas revealed a significant loss of AMBRA1 expression between the normal epidermis and the tumor growth front, in both groups of non-metastatic primary cSCCs (Figure 2B, NE H-score 123.3 vs. TGF H-score 65.99, **** $p < 0.0001$) and metastatic primary cSCCs (Figure 2C, NE H-score 133.0 vs. TGF H-score 62.09, **** $p < 0.0001$). This consistent loss of AMBRA1 expression in the tumor growth front, regardless of metastatic outcome, suggests that the loss of AMBRA1 may be associated with cSCC carcinogenesis rather than a predictor of metastatic potential.

Given that *t*-test-based statistical analysis is not an optimal test for determining prognostic ability, ROC analysis was subsequently undertaken to assess the prognostic potential of cytoplasmic AMBRA1 expression in each defined histological area of interest. Results revealed the area with the highest AUC value was the tumor growth front, with an AUC of 0.5522 (Figure 2D), a value ordinarily considered a poor prognostic indicator.²⁵ This suggests that AMBRA1 expression in the tumor growth front alone is unable to predict metastatic outcome. Moreover, Kaplan–Meier analysis of 68 cSCCs stratified as high or low risk by a tumor-growth front AMBRA1 H-score of <59.740 , did not reveal any significant difference in metastasis-free

survival over 5 years, further confirming the inability of AMBRA1 expression in the cSCC tumor growth front alone, to predict tumor metastatic potential (Figure 2E).

As with AMBRA1 expression, mean cytoplasmic H-scores for SQSTM1 expression were derived in the normal epidermis, peritumoral epidermis, tumor mass, and tumor growth front of 53 non-metastatic and 15 metastatic cSCCs. Statistical analysis of changes in expression revealed an increase in cytoplasmic SQSTM1 expression in the tumor mass and tumor growth front compared to expression in the normal epidermis and peritumoral epidermis, in both metastatic and non-metastatic cSCCs (data not shown). Subsequent ROC curve analysis of cytoplasmic SQSTM1 expression in the peritumoral epidermis, tumor mass, and tumor growth front revealed expression in the peritumoral epidermis as the area with the highest AUC (Figure 3D, 0.6352), surprising, given that *t*-test analysis did not demonstrate any significant difference in expression between the normal epidermis and peritumoral epidermis in both metastatic and non-metastatic cSCC cases (Figure 3B,C). Subsequent, Kaplan–Meier analysis of the 68 cSCCs stratified on the basis of a SQSTM1 H-score in the peritumoral epidermis of <20.010 did not reveal any significant difference in 5-year metastasis-free survival (Figure 3E). Collectively these data

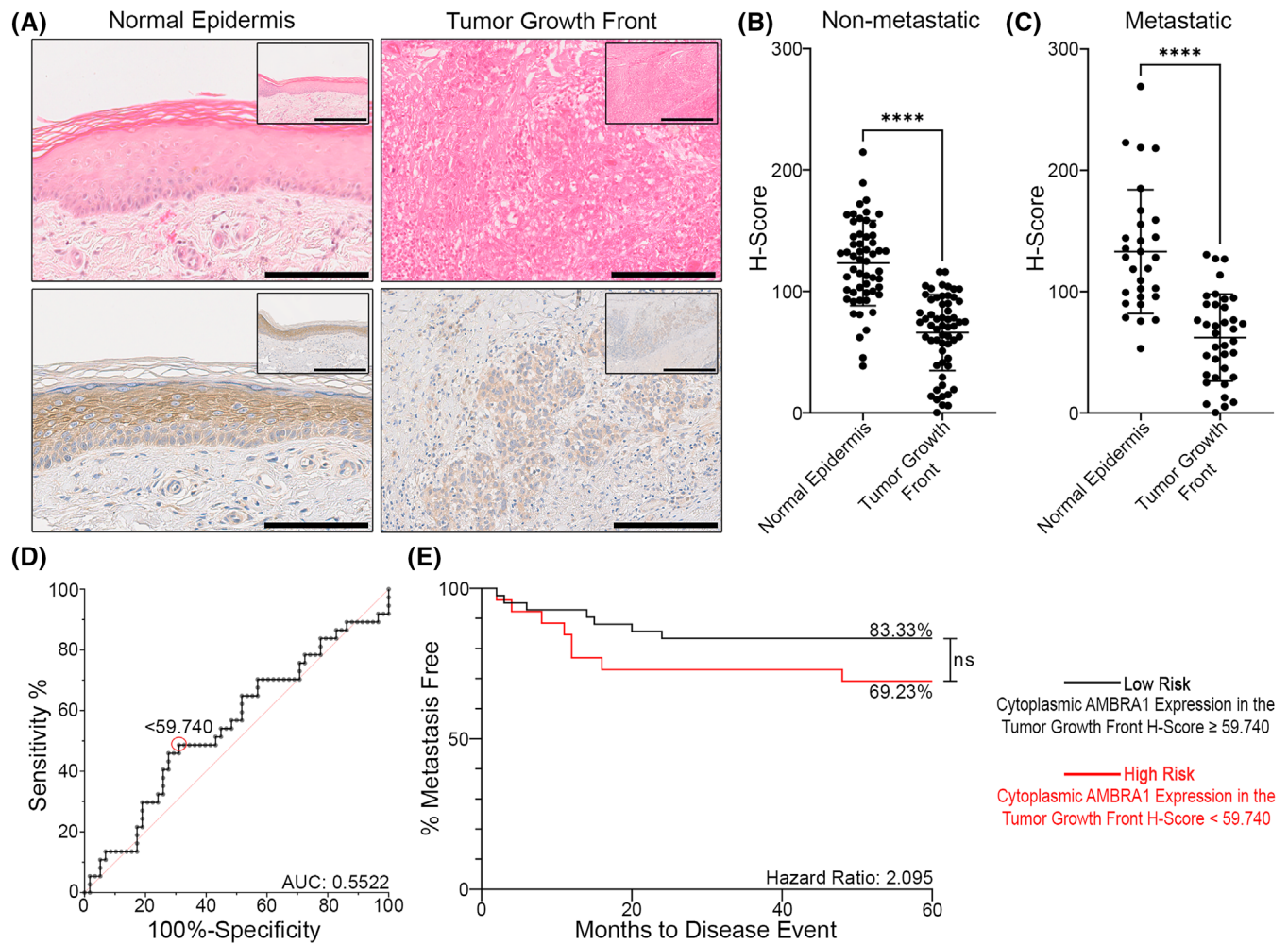


FIGURE 2 Cytoplasmic AMBRA1 expression is lost during cutaneous squamous cell carcinoma (cSCC) carcinogenesis regardless of metastatic outcome. (A) Representative hematoxylin and eosin and immunohistochemical images of cytoplasmic AMBRA1 expression in the normal epidermis and tumor growth front of a cSCC. Images were taken using bright-field microscopy at a magnification of $\times 20\times$, with a $\times 10$ insert in the right corner. Scale bars = 50 μ m. (B) Scatter graph representing the cytoplasmic AMBRA1 H-score in the normal epidermis (n = 55) and tumor growth front (n = 58) of all primary cSCCs that did not progress to metastasis. Horizontal bars represent the mean \pm SD H-score for each group. Statistics acquired by Mann-Whitney test (****p < 0.0001). (C) Scatter graph representing the cytoplasmic AMBRA1 H-score in the normal epidermis (n = 29) and tumor growth front (n = 37) of all primary cSCCs that did progress to metastasis. Horizontal bars represent the mean \pm SD H-score for each group. Statistics acquired by unpaired t-test (****p < 0.0001). (D) Receiver operator characteristic curve for prediction of cSCC metastasis based on the cytoplasmic AMBRA1 H-score in the tumor growth front of all primary cSCC tumors (n = 95). The AMBRA1 H-score with the highest specificity and sensitivity is highlighted by a red circle. (E) Kaplan-Meier survival analysis representing 60-month metastasis-free survival in 68 primary cSCC tumors stratified as low-risk (n = 42) and high-risk (n = 26) groups based on cytoplasmic AMBRA1 expression in the tumor growth front. Statistics acquired by Mantel-Cox log rank test and Mantel-Haenszel test (ns = non-significant).

suggest peritumoral epidermis SQSTM1 expression alone is unable to identify cSCCs at risk of metastasis.

3.2 | Combined peritumoral SQSTM1 and tumor growth front AMBRA1 expression identifies high-risk patient subsets with poorly differentiated cSCC

Given that both cytoplasmic AMBRA1 and SQSTM1 expression alone were unable to stratify cSCC patients according to metastatic outcomes, the prognostic potential of combining these two protein

markers was investigated. Kaplan-Meier analysis of all cSCC tumors was performed, stratifying tumors into high- or low-risk subsets based on the previously identified H-score values for AMBRA1 and SQSTM1. High-risk status was defined on the basis of a tumor growth front cytoplasmic AMBRA1 H-score of <59.740 and a peritumoral epidermis cytoplasmic SQSTM1 H-score of <20.010 , with low-risk status defined as an H-score higher than or equal to <59.740 or <20.010 for AMBRA1 or SQSTM1, respectively. Whilst unable to stratify all cSCCs according to metastatic potential (Figure S3A), sub-cohort analysis stratifying tumors by differentiation status (well, moderately, and poorly differentiated cSCCs) revealed the combined

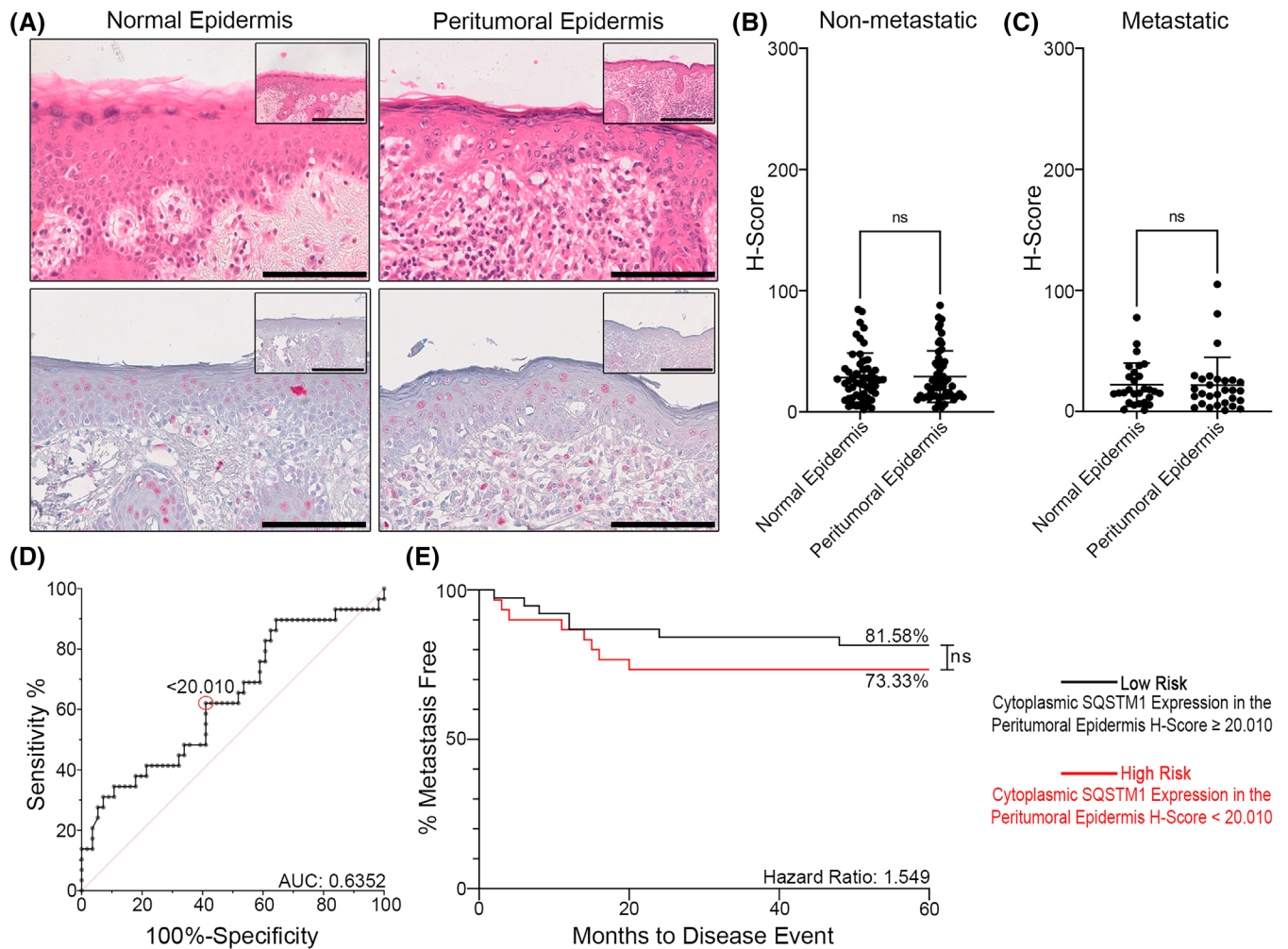


FIGURE 3 Cytoplasmic SQSTM1 expression is unchanged between the normal epidermis and the peritumoral epidermis of cutaneous squamous cell carcinomas (cSCCs). (A) Representative hematoxylin and eosin and immunohistochemical images of cytoplasmic SQSTM1 expression in the normal epidermis and peritumoral epidermis of a cSCC. Images were taken using bright-field microscopy at a magnification of $\times 20$, with a $\times 10$ insert in the right corner. Scale bars = 50 μm . (B) Scatter graph representing the cytoplasmic SQSTM1 H-score in the normal epidermis ($n = 54$) and peritumoral epidermis ($n = 56$) of all primary cSCCs that did not progress to metastasis. Horizontal bars represent the mean \pm SD H-score for each group. Statistics acquired by Mann-Whitney test (ns = non-significant). (C) Scatter graph representing the cytoplasmic SQSTM1 H-score in the normal epidermis ($n = 28$) and peritumoral epidermis ($n = 29$) of all primary cSCCs that did progress to metastasis. Horizontal bars represent the mean \pm SD H-score for each group. Statistics acquired by Mann-Whitney test (ns = non-significant). (D) Receiver operator characteristic curve for prediction of cSCC metastasis based on the cytoplasmic SQSTM1 H-score in the peritumoral epidermis of all primary cSCC tumors ($n = 85$). The SQSTM1 H-score with the highest specificity and sensitivity is highlighted by a red circle. (E) Kaplan-Meier survival analysis representing 60-month metastasis-free survival in 68 primary cSCC tumors stratified as low-risk ($n = 38$) and high-risk ($n = 30$) groups based on cytoplasmic SQSTM1 expression in the peritumoral epidermis. Statistics acquired by Mantel-Cox log rank test and Mantel-Haenszel test (ns = non-significant).

expression of AMBRA1 in the tumor growth front and SQSTM1 expression in the peritumoral epidermis identified poorly differentiated cSCCs at higher risk of metastasis (Figure 4, $*p < 0.05$), with a hazard ratio of 20.52, a positive predictive value of 40.0%, a negative predictive value of 81.0%, a sensitivity of 26.7% and a specificity of 88.68%. Conversely, the combined expression of these biomarkers did not reveal any significant association with metastatic potential in either well or moderately differentiated cSCC tumors (Figure S3B,C). Interestingly however, loss of cytoplasmic AMBRA1 in the tumor growth front and cytoplasmic SQSTM1 in the peritumoral epidermis

in a subcohort of 44 poor and moderately differentiated cSCCs with a histological subcompartment tending toward a less-differentiated phenotype also demonstrated a trend for identifying tumors at higher risk of metastasis within 5 years of primary tumor development (Figure S4, hazard ratio: 3.33).

Taken together, these data suggest that a combined cytoplasmic AMBRA1 H-score of < 59.740 in the tumor growth front and a cytoplasmic SQSTM1 H-score of < 20.010 in the peritumoral epidermis identify patients with high-risk poorly differentiated cSCCs.

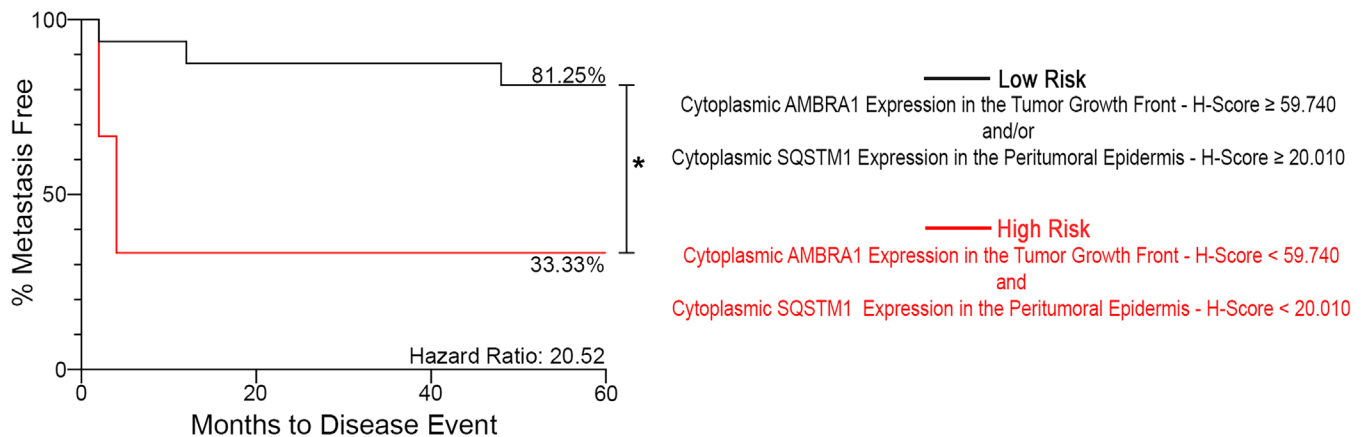


FIGURE 4 Cytoplasmic AMBRA1 expression in the tumor growth front region and cytoplasmic SQSTM1 expression in the peritumoral epidermis region is a predictor of metastasis in poorly differentiated cutaneous squamous cell carcinomas (cSCC) tumors. Kaplan–Meier survival analysis representing 60-month metastasis-free survival in 19 poorly differentiated primary cSCC tumors stratified as low-risk ($n = 16$) and high-risk ($n = 3$) groups based on cytoplasmic AMBRA1 expression in the tumor growth front region and cytoplasmic SQSTM1 expression in the peritumoral epidermis. Statistics acquired by Mantel–Cox log rank test and Mantel–Haenszel test ($*p < 0.05$).

4 | DISCUSSION

The initial investigation into the potential for AMBRA1 as a biomarker for cSCC metastasis revealed a significant loss of expression in the tumor growth front as compared with the normal epidermis, regardless of metastatic outcome, suggesting that loss of AMBRA1 expression associated with initial cSCC carcinogenesis, rather than as a prerequisite for acquiring invasive potential. This is consistent with previous work demonstrating a role for autophagy in epidermal differentiation, suggesting the loss of AMBRA1 promotes a dedifferentiated and proliferative cell state, critical for carcinogenesis and further supported by our observation that loss of AMBRA1 expression alone is unable to identify high-risk tumor subsets.¹¹ Nevertheless, although reduced, our data suggest AMBRA1 expression levels are sufficient to evoke autophagy to allow for continued cSCC cell survival during invasion, yet are not sufficient enough to encourage epidermal differentiation, which would prevent tumor cell proliferation, tumor invasion, and metastasis.

Surprisingly, the investigation into the potential of SQSTM1 as a prognostic biomarker revealed expression in the peritumoral epidermis as the area with the highest prognostic power. SQSTM1 has been implicated in several intratumoral and extratumoral signaling pathways, including contributing to increased cell migration, as well as metabolic and tumor microenvironment reprogramming.^{20,21,26–28} Given an H-score of <20.010 identified cSCC cases at higher risk of metastasis, this suggests that a near total suppression of SQSTM1 is associated with a higher risk of developing metastatic disease. Recent work has demonstrated that autophagic function has been linked to the maintenance of intestinal epithelium tight junctional complexes, and thus, suppression of SQSTM1 expression and activity may weaken epidermal integrity and allow for cSCC cell epidermal detachment and invasion.²⁹ However, as with AMBRA1 expression in the tumor growth front, peritumoral epidermis expression of SQSTM1

alone was also unable to identify cSCC cases at high risk of metastasis, suggesting that whilst this potential reduction in epidermal integrity contributes to invasion, it is not sufficient to promote this alone.

However, when combining an H-score <59.740 for the expression of AMBRA1 in the tumor growth front with an H-score <20.010 for the expression of SQSTM1 expression in the peritumoral epidermis, this identified high-risk cSCC patient subsets with poorly differentiated tumors, with a similar, non-significant trend for the identification of any cSCC with a component tending toward a less-differentiated phenotype. It is worth noting that neither AMBRA1 nor SQSTM1 expression significantly correlated with either BWH stage or immune status (data not shown), further suggesting any alteration to their expression is not linked to these established risk factors.

Multiple prognostic biomarkers have been proposed for cSCC, yet few have been subjected to further validation.^{30–32} Recently, however, an encouraging gene expression profile (GEP) test has been developed, which classifies the risk of cSCC metastasis based on the expression of 40 genes in the primary tumor through the use of a multianalyte algorithmic.¹⁰ However, given the expense of GEP tests and the tissue requirements, the use of combined AMBRA1/SQSTM1 expression presents an additional promising immunohistochemical-based alternative for the identification of high-risk poorly differentiated cSCCs that would fit seamlessly into current clinical diagnostic pathways.

Whilst the basis of these studies relies on the detailed quantification of AMBRA1/SQSTM1 expression, it has also identified the general trend that loss of expression of both markers in the tumor growth front and peritumoral epidermis is predictive for poorly differentiated cSCC. Future work is therefore focused on refining the quantification of these proteins to provide an immunohistochemically based prognostic biomarker that can be used on both an AI-driven analysis platform (via the addition of an extension onto the existing departmental limbs systems, which now exist in most diagnostically digitized

pathology departments), as well as via light microscopy analysis, as per the traditional diagnostic practice. Through the acquisition of larger cSCC tissue cohorts, we aim to quantifiably determine further diagnostically relevant staining patterns and their potential categorization into a graded system (rather than a binary system), as seen for example with HER-2 staining.³³ In addition, we endeavor to refine our assays, therefore assisting us with the potential reduction in the number of visual fields required for an adequate assessment of the tumor growth front. Both approaches would provide cheaper and adaptable options to be harnessed by existing laboratory systems, as compared to alternative GEP tests, which are more costly and require outsourcing.

In summary, this proof of concept study suggests the combined loss of cytoplasmic AMBRA1 and SQSTM1 expression in the tumor growth front and peritumoral epidermis, respectively, as a putative prognostic biomarker to identify subsets of patients with poorly differentiated cSCCs at increased risk of metastasis, warranting further biomarker discovery and validation analysis in additional powered independent tissue cohorts.

ACKNOWLEDGMENT

None.

CONFLICT OF INTEREST STATEMENT

Penny Lovat is the Chief Scientific Officer for AMLo Biosciences. Other authors declare no conflict of interest.

DATA AVAILABILITY STATEMENT

The data that support the findings of this study are available from the corresponding author upon reasonable request.

ORCID

Michael H. Alexander  <https://orcid.org/0000-0002-7196-4101>

Tom Ewen  <https://orcid.org/0000-0001-9178-9614>

REFERENCES

- Yang DD, Borsky K, Jani C, et al. Trends in keratinocyte skin cancer incidence, mortality and burden of disease in 33 countries between 1990 and 2017. *Br J Dermatol.* 2023;188(2):237-246. doi:10.1093/bjd/ljac064
- Simonacci F, Bertozzi N, Grieco MP, Grignaffini E, Rapisio E. Surgical therapy of cutaneous squamous cell carcinoma: our experience. *Acta Biomed.* 2018;89(2):242-248. doi:10.23750/abm.v89i2.6189
- van Lee CB, Roorda BM, Wakkee M, et al. Recurrence rates of cutaneous squamous cell carcinoma of the head and neck after Mohs micrographic surgery vs. standard excision: a retrospective cohort study. *Br J Dermatol.* 2019;181(2):338-343. doi:10.1111/bjd.17188
- Rabinowitz G, Migden MR, Schlessinger TE, et al. Evidence-based consensus recommendations for the evolving treatment of patients with high-risk and advanced cutaneous squamous cell carcinoma. *JID Innov.* 2021;1(4):100045. doi:10.1016/j.xjidi.2021.100045
- Que SKT, Zwald FO, Schmults CD. Cutaneous squamous cell carcinoma: incidence, risk factors, diagnosis, and staging. *J Am Acad Dermatol.* 2018;78(2):237-247. doi:10.1016/j.jaad.2017.08.059
- Inman GJ, Wang J, Nagano A, et al. The genomic landscape of cutaneous SCC reveals drivers and a novel azathioprine associated mutational signature. *Nat Commun.* 2018;9(1):3667. doi:10.1038/s41467-018-06027-1
- Azimi A, Lo K, Kim J, Fernandez-Penas P. Investigating proteome changes between primary and metastatic cutaneous squamous cell carcinoma using SWATH mass spectrometry. *J Dermatol Sci.* 2020;99(2):119-127. doi:10.1016/j.jdermsci.2020.06.012
- Azimi A, Yang P, Ali M, et al. Data independent acquisition proteomic analysis can discriminate between actinic keratosis, Bowen's disease, and cutaneous squamous cell carcinoma. *J Invest Dermatol.* 2020;140(1):212-222.e11. doi:10.1016/j.jid.2019.06.128
- South AP, Purdie KJ, Watt SA, et al. NOTCH1 mutations occur early during cutaneous squamous cell carcinogenesis. *J Invest Dermatol.* 2014;134(10):2630-2638. doi:10.1038/jid.2014.154
- Wysong A, Newman JG, Covington KR, et al. Validation of a 40-gene expression profile test to predict metastatic risk in localized high-risk cutaneous squamous cell carcinoma. *J Am Acad Dermatol.* 2021;84(2):361-369. doi:10.1016/j.jaad.2020.04.088
- Ellis R, Tang D, Nasr B, et al. Epidermal autophagy and beclin 1 regulator 1 and loricrin: a paradigm shift in the prognostication and stratification of the American Joint Committee on Cancer stage I melanomas. *Br J Dermatol.* 2020;182(1):156-165. doi:10.1111/bjd.18086
- Johnson CE, Tee AR. Exploiting cancer vulnerabilities: mTOR, autophagy, and homeostatic imbalance. *Essays Biochem.* 2017;61(6):699-710. doi:10.1042/ebc20170056
- Mahanty S, Dakappa SS, Shariff R, et al. Keratinocyte differentiation promotes ER stress-dependent lysosome biogenesis. *Cell Death Dis.* 2019;10(4):269. doi:10.1038/s41419-019-1478-4
- Rossiter H, König U, Barresi C, et al. Epidermal keratinocytes form a functional skin barrier in the absence of Atg7 dependent autophagy. *J Dermatol Sci.* 2013;71(1):67-75. doi:10.1016/j.jdermsci.2013.04.015
- Di Bartolomeo S, Corazzari M, Nazio F, et al. The dynamic interaction of AMBRA1 with the dynein motor complex regulates mammalian autophagy. *J Cell Biol.* 2010;191(1):155-168.
- Labus M, Ellis R, Ewen T, et al. AMBLor: a prognostic and stratifying biomarker for adjuvant immunotherapy of AJCC stage II melanomas. *J Clin Oncol.* 2020;38(15_suppl):e22094. doi:10.1200/JCO.2020.38.15_suppl.e22094
- Ellis RA, Horswell S, Ness T, et al. Prognostic impact of p62 expression in cutaneous malignant melanoma. *J Invest Dermatol.* 2014;134(5):1476-1478. doi:10.1038/jid.2013.497
- Lamark T, Svenning S, Johansen T. Regulation of selective autophagy: the p62/SQSTM1 paradigm. *Essays Biochem.* 2017;61(6):609-624. doi:10.1042/ebc20170035
- Klionsky DJ, Abdel-Aziz AK, Abdelfatah S, et al. Guidelines for the use and interpretation of assays for monitoring autophagy (4th edition). *Autophagy.* 2021;17(1):1-382. doi:10.1080/15548627.2020.1797280
- Kang JI, Kim DH, Sung KW, et al. p62-induced cancer-associated fibroblast activation via the Nrf2-ATF6 pathway promotes lung tumorigenesis. *Cancers.* 2021;13(4):864. doi:10.3390/cancers13040864
- Reina-Campos M, Shelton PM, Diaz-Meco MT, Moscat J. Metabolic reprogramming of the tumor microenvironment by p62 and its partners. *Biochim Biophys Acta.* 2018;1870(1):88-95. doi:10.1016/j.bbcan.2018.04.010
- Brierley JD, Gospodarowicz MK, Wittekind C. *Skin tumours. TNM Classification of Malignant Tumours.* 8th ed. Wiley-Blackwell; 2017:131-150.
- Cosgarea I, McConnell AT, Ewen T, et al. Melanoma secretion of transforming growth factor- β 2 leads to loss of epidermal AMBRA1 threatening epidermal integrity and facilitating tumour ulceration. *Br J Dermatol.* 2022;186(4):694-704. doi:10.1111/bjd.20889
- Meyerholz DK, Beck AP. Principles and approaches for reproducible scoring of tissue stains in research. *Lab Invest.* 2018;98(7):844-855. doi:10.1038/s41374-018-0057-0

25. Kamarudin AN, Cox T, Kolamunnage-Dona R. Time-dependent ROC curve analysis in medical research: current methods and applications. *BMC Med Res Methodol*. 2017;17(1):53. doi:[10.1186/s12874-017-0332-6](https://doi.org/10.1186/s12874-017-0332-6)
26. Linares JF, Duran A, Reina-Campos M, et al. Amino acid activation of mTORC1 by a PB1-domain-driven kinase complex cascade. *Cell Rep*. 2015;12(8):1339-1352. doi:[10.1016/j.celrep.2015.07.045](https://doi.org/10.1016/j.celrep.2015.07.045)
27. Sun X, Ou Z, Chen R, et al. Activation of the p62-Keap1-NRF2 pathway protects against ferroptosis in hepatocellular carcinoma cells. *Hepatology*. 2016;63(1):173-184. doi:[10.1002/hep.28251](https://doi.org/10.1002/hep.28251)
28. Zhang T, Guo L, Wang Y, Yang Y. Macroautophagy regulates nuclear NOTCH1 activity through multiple p62 binding sites. *IUBMB Life*. 2018;70(10):985-994. doi:[10.1002/iub.1891](https://doi.org/10.1002/iub.1891)
29. Foerster EG, Mukherjee T, Cabral-Fernandes L, Rocha JDB, Girardin SE, Philpott DJ. How autophagy controls the intestinal epithelial barrier. *Autophagy*. 2022;18(1):86-103. doi:[10.1080/15548627.2021.1909406](https://doi.org/10.1080/15548627.2021.1909406)
30. Cañueto J, Cardenoso-Álvarez E, Cosano-Quero A, et al. The expression of podoplanin is associated with poor outcome in cutaneous squamous cell carcinoma. *J Cutan Pathol*. 2017;44(2):144-151. doi:[10.1111/cup.12859](https://doi.org/10.1111/cup.12859)
31. Campos MA, Macedo S, Fernandes M, et al. TERT promoter mutations are associated with poor prognosis in cutaneous squamous cell carcinoma. *J Am Acad Dermatol*. 2019;80(3):660-669.e6. doi:[10.1016/j.jaad.2018.08.032](https://doi.org/10.1016/j.jaad.2018.08.032)
32. Xu R, Cai M-Y, Luo R-Z, Tian X, Han J-D, Chen M-K. The expression status and prognostic value of cancer stem cell biomarker CD133 in cutaneous squamous cell carcinoma. *JAMA Dermatol*. 2016;152(3):305-311. doi:[10.1001/jamadermatol.2015.3781](https://doi.org/10.1001/jamadermatol.2015.3781)
33. Ahn S, Woo JW, Lee K, Park SY. HER2 status in breast cancer: changes in guidelines and complicating factors for interpretation. *J Pathol Transl Med*. 2020;54(1):34-44. doi:[10.4132/jptm.2019.11.03](https://doi.org/10.4132/jptm.2019.11.03)

SUPPORTING INFORMATION

Additional supporting information can be found online in the Supporting Information section at the end of this article.

How to cite this article: Alexander MH, Cousins WJ, Ewen T, South AP, Lovat P, Stefanos N. The combined immunohistochemical expression of AMBRA1 and SQSTM1 identifies patients with poorly differentiated cutaneous squamous cell carcinoma at risk of metastasis: A proof of concept study. *J Cutan Pathol*. 2024;1-9. doi:[10.1111/cup.14590](https://doi.org/10.1111/cup.14590)